Journal of Applied Physics

Interface conductance modal analysis of a crystalline Si-amorphous SiO_2 interface

Cite as: J. Appl. Phys. **125**, 135102 (2019); https://doi.org/10.1063/1.5085328
Submitted: 11 December 2018 . Accepted: 19 March 2019 . Published Online: 02 April 2019

Kiarash Gordiz, Murali Gopal Muraleedharan, and Asegun Henry

Journal of Applied Physics ARTICLE scitation.org/journal/jap

Interface conductance modal analysis of a crystalline Si-amorphous SiO_2 interface

Cite as: J. Appl. Phys. **125**, 135102 (2019); doi: 10.1063/1.5085328
Submitted: 11 December 2018 · Accepted: 19 March 2019 ·
Published Online: 2 April 2019

Kiarash Gordiz,[1,a)] Murali Gopal Muraleedharan,[2,a)] and Asegun Henry[1,b)]

AFFILIATIONS

[1]Department of Mechanical Engineering, Massachusetts Institute of Technology, Cambridge, Massachusetts 02139, USA
[2]School of Aerospace Engineering, Georgia Institute of Technology, Atlanta, Georgia 30332, USA

[a)]**Contributions:** K. Gordiz and M. G. Muraleedharan contributed equally to this work.
[b)]**Author to whom correspondence should be addressed:** ase@mit.edu

ABSTRACT

We studied the modal contributions to heat conduction across an interface between crystalline Si and amorphous SiO_2, using the interface conductance modal analysis (ICMA) method. Our results show that >70% of the thermal interface conductance (TIC) arises from the extended modes. Using ICMA, we could also determine the contribution of interfacial modes to the TIC. Interestingly, we observed that although the number of these modes is <5% of all modes, interfacial modes contribute significantly to the TIC (>15%). Such an observation shows the non-negligible role of localized modes in facilitating heat conduction across systems with interfaces between dissimilar materials, specifically in a system that is straightforward to fabricate and study experimentally. Our observations suggest that neglecting the contribution of localized modes would be an oversimplification of the actual mechanisms at play. Determining the individual mode contributions is therefore of vital importance, since these values are directly utilized in predicting the temperature dependent TIC, which is important to silicon on insulator technologies with a myriad of applications within microelectronics and optoelectronics.

INTRODUCTION

Silicon (Si) on insulator (SOI) technology is widely employed in microelectronics, where an oxide layer, i.e., amorphous silica (SiO_2),[1] separates the top active Si layer from the bottom bulk Si handle substrate. Although the introduction of the SiO_2 layer greatly enhances the electronic performance of the system by diminishing the short-channel effects[2] and parasitic capacitance,[3,4] its presence adds a barrier to the extraction of heat from devices. In fact, the limits on heat dissipation to this day remain the main barrier to achieving higher operational speeds in micro/nanoelectronics.[5,6]

The main barriers to heat dissipation in SOI devices are largely attributed to the thermal resistances (i) in the bulk of the SiO_2 layer and (ii) at the interface of crystalline (c) Si and amorphous (a) SiO_2 layers (c-Si/a-SiO_2 interface).[7] To assess the relative importance of these thermal resistances across the c-Si/a-SiO_2 interface, we used the interface conductance modal analysis (ICMA) approach[8–10] to evaluate the thermal interface conductance (TIC). TIC, denoted by G, relates the heat flux through the interface (Q) to the temperature difference at the interface (ΔT), where $Q = G\Delta T$. Our calculations show that at a typical operating temperature of 600 K,[11] the TIC is ~0.65 GW/m^2 K. The thermal resistance introduced to the system by this value of TIC is equal to that of a 2 nm a-SiO_2 layer with a thermal conductivity of 1.2 W/m K.[12] Since the thickness for a typical industry-standard buried oxide layer in an SOI wafer is ~50 nm,[1] this shows that the TIC for a c-Si/a-SiO_2 interface is so high that it contributes a negligible resistance to heat conduction in SOI technology. However, since the interatomic potential in our ICMA calculations was not derived or fit to first-principles calculations,[13,14] our prediction that the TIC is this high is not conclusive, and experiments are still needed to confirm if this prediction is correct.

Recently, Kimling *et al.*[15] experimentally measured the TIC across the c-Si/a-SiO_2 interface to be greater than 0.6 GW/m^2 K at room temperature. Considering that the TIC across many interfaces increases with temperature,[16–18] the room-temperature TIC value obtained by Kimling *et al.*[15] can potentially be extrapolated to a value larger than 0.6 GW/m^2 K at the operating temperature of 600 K,[11] which supports our conjecture about the negligibility of the thermal resistance caused by the c-Si/a-SiO_2 interface. It is

therefore interesting to study more deeply how such a high TIC can arise at an interface between such dissimilar materials, namely, one amorphous and one crystalline. Specifically, it will be interesting to investigate more deeply whether localized modes play any appreciable role. If so, this system can become a useful example case that is straightforward to fabricate and characterize, thereby enabling higher fidelity comparisons between theory and experiment, and may help establish more conclusively whether localized modes are non-negligible.

In addition to experimental observations, the large value of TIC across the c-Si/a-SiO_2 interface has also been reported in other computational studies.[7,19–22] Mahajan *et al.*,[19] Lampin *et al.*,[20] and Chen *et al.*[23] have employed the nonequilibrium molecular dynamics (NEMD) method to quantify the magnitude of temperature discontinuity at the interface of c-Si/a-SiO_2, and by knowing the applied heat flux Q, they used the definition of G ($Q = G\Delta T$) to determine the TIC. Stanley and co-workers[21,22] used a modified approach to nonequilibrium heat conduction implemented in a first-principles molecular dynamics (MD) simulation to capture the TIC at the c-Si/a-SiO_2 interface. However, none of the aforementioned studies analyzed the modal contributions to the TIC. Only Deng *et al.*[7] quantified modal contributions to the heat conduction across a c-Si/a-SiO_2 interface by employing the wave packet (WP) dynamics approach. However, one drawback of using WP dynamics for modal analysis is the inherently very low temperature of the system during the simulation and therefore the inability to study moderate temperatures and temperature dependent effects.[9,24] At such low temperatures, even if anharmonic interatomic potentials are used in the simulations, the vibrational amplitudes are so small that fully incorporating the anharmonic effects that are naturally present at room temperature may not be possible.[25,26] Apart from the anharmonic effects, in the WP analysis by Deng *et al.*,[7] the modal contributions were ascribed to the propagating modes on the Si side (i.e., the modes from the crystalline Si dispersion curve). Such a treatment of vibrational modes neglects any possible contribution to TIC by nonpropagating and/or localized modes in the system and is an oversimplification of the problem, in light of the work by Gordiz and Henry.[9] In their paper, they showed systematically that utilizing the modes associated with only one side of the interface is incorrect, since it leads to an erroneous aliasing of the contributions. Thus, it is critical that a study of the modal contributions to TIC be based on the modes of the full combined system, which can hybridize, and induce localization. In fact, there is already some experimental evidence to suggest that localized modes exist at the Si/SiO_2 interface, based on electron microscopy.[27] Furthermore, localized modes have been previously shown[28–30] with MD to play an important role in other interfacial systems. The problem, however, is that the studies of other systems have involved material pairs that can be quite challenging to fabricate. Nonetheless, here, we have chosen a more straightforward system to fabricate, and thus it is anticipated that this system can serve as a test platform for assessing the validity/accuracy of different methods. In general, it is important to determine the contributions of all modes of vibration in the system, including the nonpropagating and localized interfacial modes, so that quantum corrections can be applied[9,31] and the physics can be better understood. Such an investigation is the focus of the study presented herein.

METHODS

To determine the modal contributions to the TIC of a c-Si/a-SiO_2 interface by all types of vibrations in the system, including the localized ones, we used the ICMA approach introduced by Gordiz and Henry.[8,9] ICMA is evaluated using MD and, therefore, it can fully include anharmonicity. In addition, since ICMA is ultimately based on the fluctuation dissipation theorem, it expresses the interactions between modes from a correlation perspective, through which one can elucidate the contributions from localized modes. Using the correlation picture, ICMA presents a different interpretation of interfacial heat transfer than methods such as WP dynamics that are based on the phonon gas model (PGM) and use the scattering picture to describe the interfacial conduction of heat, which is intrinsically tied to the notion of a transmission probability.

Considering these conceptual differences, for this study, we used ICMA and equilibrium MD to calculate the modal contributions to TIC. The ICMA formulation has been fully explained in previous studies by Gordiz and Henry.[8,9] It should be noted that ICMA can also be used in NEMD simulations, which can be utilized to capture the nonequilibrium distribution of phonons around the interface, which has been shown to be an important effect in interfacial heat transfer by a recent study.[32] Periodic boundary conditions (BCs) were applied to all three Cartesian coordinates, and a time step of 0.15 fs was chosen for the MD simulations. It should be noted that by using periodic boundary conditions, the system would be a representation of a superlattice structure. However, even though the periodic boundaries equate to a superlattice, the behavior observed in the EMD simulations is independent of the fact that the structure is repeated. The reason is that in our considered structures only one unit cell belonging to the superlattice structure is being simulated, which restricts the actual modes belonging to a periodic superlattice structure (such as the collective modes) from existing in the system. Therefore, the collective modes associated with the repeat units of the superlattice do not exist in this simulation, as they are not part of the allowed modes of vibration[33] in such a short structure. To understand this more deeply, consider another example where one could do a MD simulation of a single unit cell in a material such as crystalline silicon. Such a simulation would consist of only two atoms. Even though periodic boundary conditions can be exploited to calculate modes of an infinite structure as is done in the lattice dynamics (LD) formalism, only 6 modes (i.e., $3N = 3 \times 2$) exist in the two atom MD simulation. Similarly, the modes associated with multiple periods do not exist in our calculations that contain only a single period. Consequently, our results do not include superlattice modes. Nevertheless, we have checked this effect by considering the total values of thermal interface conductance when both periodic and nonperiodic boundary conditions normal to the interface are considered in the simulations, and the difference between the two are less than 5% (see Fig. 1). Therefore, the system with periodic boundaries is representative of the behaviors that would occur for a single interface.

To describe the atomic interactions, we used the Tersoff interatomic potential.[34] The direction of the Si crystal structure normal to the interface is [100]. Moreover, for the Si side, we used a $4 \times 4 \times 13$ unit-cell structure (~7 nm length) comprising 1664

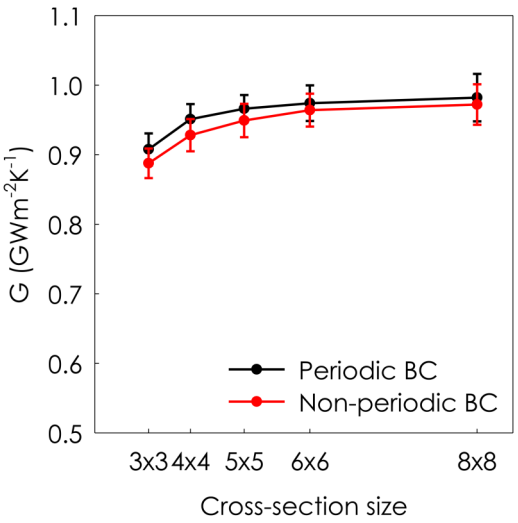

FIG. 1. Total TIC values for different cross-section sizes calculated with periodic and nonperiodic boundary conditions (BCs) in the direction normal to the interface. All the simulations are done at 600 K, and the reported values are not quantum-corrected.

atoms. The SiO_2 side also has the same cross section and length (~7 nm length) as the Si side and is comprised of 2160 atoms. We examined the effect of larger cross sections up to 8×8 unit cells and longer systems up to 50 unit cells, and neither resulted in changes larger than 5% to the total values of TIC (see Fig. 1), which shows that all the previously reported important effects by transverse phonons[35,36] are converged in our 4×4 cross-section systems. To generate the structure for the amorphous SiO_2 side, Si and O atoms were initially placed at their crystalline positions corresponding to the cristobalite lattice. The system was then heated to a temperature above its melting point, after which it was quenched to 0 K over a 50 ns simulation time. The two sides are then brought into contact, and the entire system is annealed at 1000 K for 2 ns. This annealing procedure is required to ensure the correct positioning of atoms around their equilibrium sites.[7,37] After this step, the structures are further relaxed, based on the force and energy minimization criteria, using the General Utility Lattice Program (GULP).[38] The density of the obtained amorphous SiO_2 sides from this procedure (~2.215 g/cm^3) showed excellent agreement with the reported nominal experimental values (~2.2 g/cm^3).[39] In addition, the structures generated based on the explained procedure did not show any negative frequencies in the LD calculations. For the MD simulations, after initially relaxing the structure under the isobaric-isothermal ensemble (NPT) for 1 ns at zero pressure and at the desired simulation temperature (e.g., $T = 600\,K$), the system is further relaxed under the canonical ensemble (NVT) for another 1 ns at the desired simulation temperature. The structure is then simulated in the microcanonical (NVE) ensemble for 10 ns during which the modal contributions to the heat flux across the interface were calculated. The heat flux contributions were saved and postprocessed to calculate the mode-mode heat flux correlation functions. Statistical uncertainty, due to insufficient phase space sampling,[40] has been reduced to less than 5% by considering 5 independent ensembles. The MD simulations were performed using the Large Atomic/Molecular Massively Parallel Simulator (LAMMPS)[41] and the LD calculations were performed using GULP.[38] It should be noted that since the LD analysis in ICMA is performed on the entirety of the system,[9] ICMA is able to capture the effect of atoms far from the interface and all their corresponding modes of vibration on the interfacial heat transfer. Including the effect of all the atoms in the system, particularly the ones far away from the interface, is crucial for the correct analysis of heat transfer around interfaces, which has also been emphasized in other studies.[36,37]

RESULTS AND DISCUSSION

Based on the degree of localization of the vibrational energy, all the modes of vibration in an interfacial system can be classified into four groups of modes: (1) extended modes, (2) partially extended modes, (3) isolated modes, and (4) interfacial modes.[9] Typical examples of these modes in this c-Si/a-SiO_2 interfacial system are illustrated in Fig. 2. These modes have been calculated using LD calculations based on empirical interatomic potentials for several interfacial systems in prior studies.[9,29,37,42,43] In concept, the modes' shapes could be partially confirmed by vibrational spectroscopy and there are some existing data in the literature for this system. Recently, high-energy resolution monochromated electron energy loss spectroscopy (EELS) systems (HERMESs)[27] have shown the potential to directly detect the spatial distribution of vibrational modes in interfacial structures at a specific frequency. In HERMES, vibrational spectroscopy is combined with the spatial resolution and flexibility of the transmission electron microscope. A monochromatic electron beam is passed through a sample by advancing a probe in steps with subnanometer resolution, and the response of the material to electrons at different energies is recorded, which provides insight into how strongly (i.e., how many modes exist at that frequency) atoms at that location are vibrating at the specific frequency. When electrons couple to a vibrational mode in the sample, a prominent peak is obtained, indicating energy absorption and the presence of corresponding modes at that location.

Krivanek *et al.*[27] used HERMES to obtain the vibrational spectra of a-SiO_2. The results indicated a vibrational peak at 138 meV (33.34 THz) corresponding to Si–O bond stretching in SiO_2.[44] They also studied the spatial variation of SiO_2 phonons at the c-Si/a-SiO_2 interface. A probe of ~2 nm diameter was used, and a line scan across the interface structure with 2 nm advancement was performed by recording a spectrum for 10 s at each location. Spatial variation of phonon intensity is represented by the red dots in Fig. 3. As can be seen from Fig. 3, phonon intensity is very low on the Si side due to the lack of vibrational modes corresponding to 33.34 THz. On the SiO_2 side, the intensity has a fairly high value owing to the interaction of electrons with phonons in SiO_2 corresponding to 33.34 THz. Figure 3 shows that as the beam gets close to the interface, the signal intensity experiences a rapid increase near the interface. Using the dielectric response theory, Krivanek *et al.*[27] ascribed this observed jump at the interface to the localized vibrations in that region. Of key importance is the experimental point located at the interface, which has a higher value than that

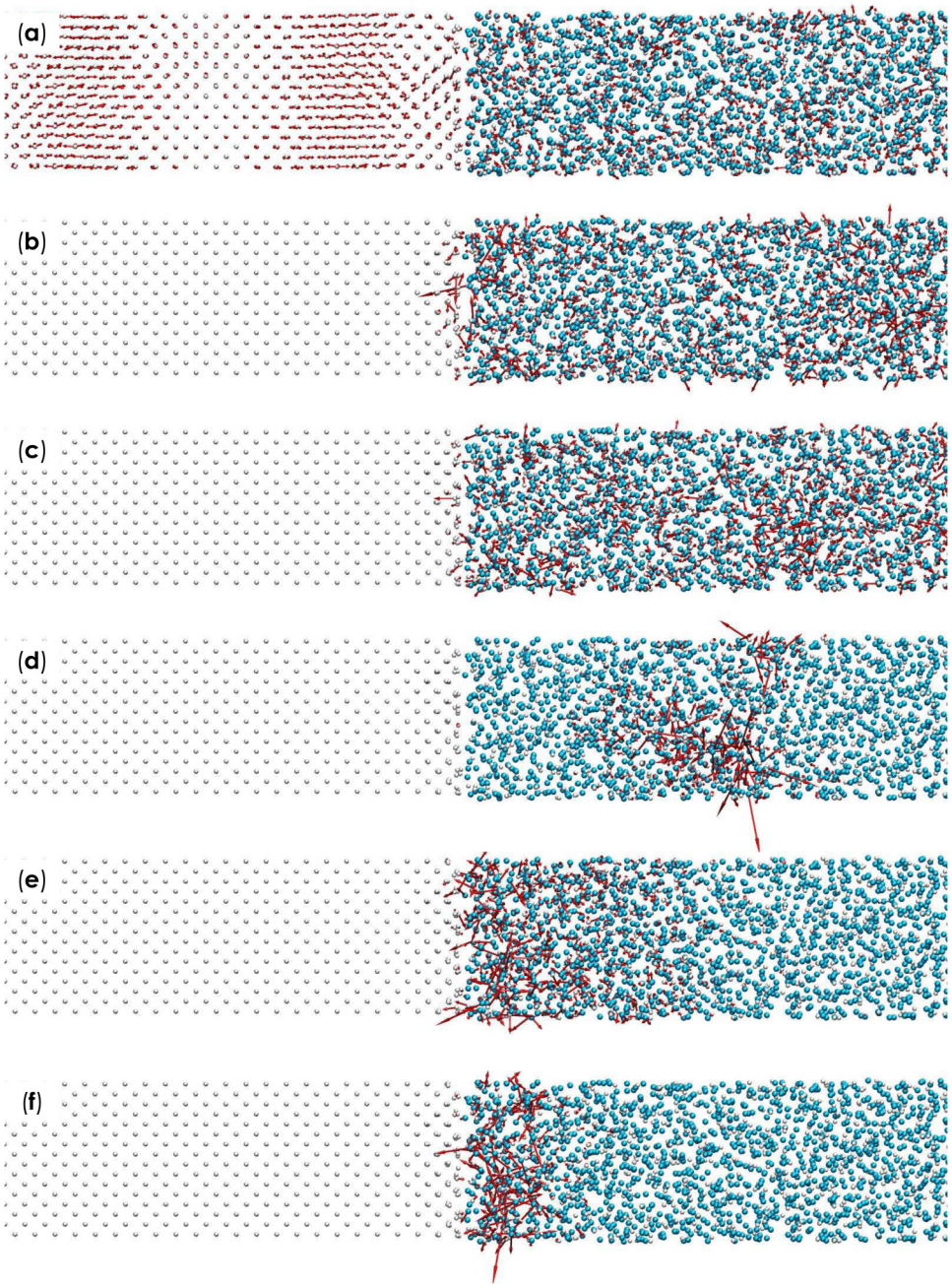

FIG. 2. Eigen vectors for different examples of the four classes of vibration present at the interface of c-Si/a-SiO_2. Si and O atoms are represented by white and cyan spheres, respectively. The included examples, the region they belong to in Fig. 4, and their frequencies are (a) the extended mode in region 1 at 5.16 THz, (b) the partially extended mode in region 2 at 23.81 THz, (c) the partially extended mode in region 4 at 33.86 THz, (d) the isolated mode in region 3 at 27.04 THz, (e) the interfacial mode in region 3 at 29.85 THz, and (f) the interfacial mode in region 5 at 32.76 THz.

obtained in the bulk of c-Si. The fact that a higher value than the bulk in c-Si was obtained indicates that some of the atoms in c-Si are actually vibrating at 33.34 THz. The reason this is significant is because the maximum frequency that atoms in c-Si vibrate is limited to less than ~16 THz.[29] Therefore, the slight increase of the signal near the interface indicates that some atoms in c-Si are able to vibrate above their normal bulk maximum frequency due to the interfacial interactions with oxygen atoms in a-SiO_2. This is noteworthy because the most widely accepted approach to modeling interfacial heat flow is to use expressions based on the Landauer formalism, which according to the principle of detailed balance require information from only one side of the interface. Most frequently, studies have used the bulk phonon properties of each material, which by definition neglect the possibility of localized interfacial modes playing an important role. Furthermore, the idea that the atoms in c-Si can vibrate above the bulk maximum

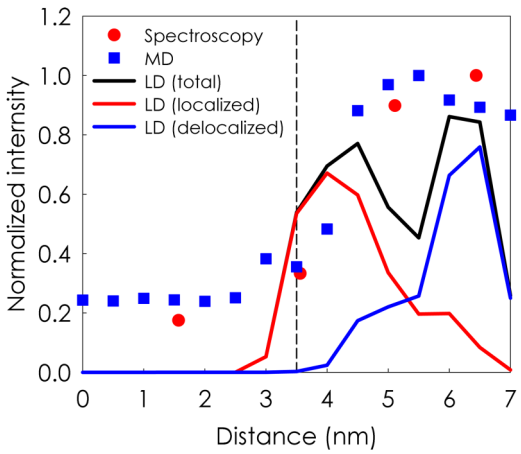

FIG. 3. Net intensity of the SiO_2 vibrational signal at 33.34 THz (138 meV) as a function of the probe position, and approximate sample thickness obtained from vibrational spectroscopy in HERMES (red dots) compared with the Gaussian weighted average of intensity obtained from MD (blue squares) and LD simulations. Total intensity calculated from LD is given as the black line, and contributions from localized and delocalized modes are represented by red and blue lines. The dashed vertical line marks the location of the Si/SiO_2 interface.

frequency is intrinsically tied to the concept of localized modes, since it must be caused by the presence of localized modes. Therefore, the reason this measurement is quite powerful is that it should be possible to make a prediction of the signal using LD, and if there is correspondence, it would offer some experimental confirmation that localized modes do in fact exist in such structures.

In light of this potential for a direct comparison with the experimental data, we used both MD and LD-based calculations to obtain the phonon intensity values across the interface and thereby distinguish localized modes from delocalized/extended modes. The comparison between our theoretically calculated phonon intensity values and the experimentally measured ones is shown in Fig. 3. The blue squares represent the Gaussian weighted average of intensities at 33.34 THz obtained from fast Fourier transform (FFT) of kinetic energy of the atoms[45] in an MD simulation at 300 K. Averaging is done in spatial bins separated by 0.5 nm, smoothed by a Gaussian weighting function with a standard deviation of 2 nm to mimic the diameter of the probe and offer the most fair comparison with the experimental data (see note 1 in the supplementary material for further details). The results in Fig. 3 show good agreement with the experimental measurements. Figure 3 also includes the Gaussian weighted average of the total harmonic potential energy evaluated at a frequency of 33.34 THz. The energy associated with localized and delocalized modes was obtained from an LD-based approach, originally introduced by Gordiz and Henry,[29] that uses the eigenvectors of the modes of vibration for the calculations (see note 2 in the supplementary material for further details). By using the LD results, we can obtain even more detail, since it allows us to partition how much of the energy at a given location can be attributed to localized modes, vs all other modes. As expected, the localized component peaks around the interface. However, what is more surprising is that the contributions from all other modes in this region are negligible, which strongly suggests that the increase in signal at the interface in the experiment is almost exclusively due to interfacial modes (i.e., as opposed to partially extended modes from the SiO_2 side that partially penetrate into c-Si). Comparisons at other frequencies are also needed to more fully confirm the interpretation herein, but the agreement between the model and the experiments is compelling.

Figure 4(a) shows the total and the partial density of states (DOS) for each class of modes. As expected, the low frequency modes of vibration are predominantly extended modes, and most

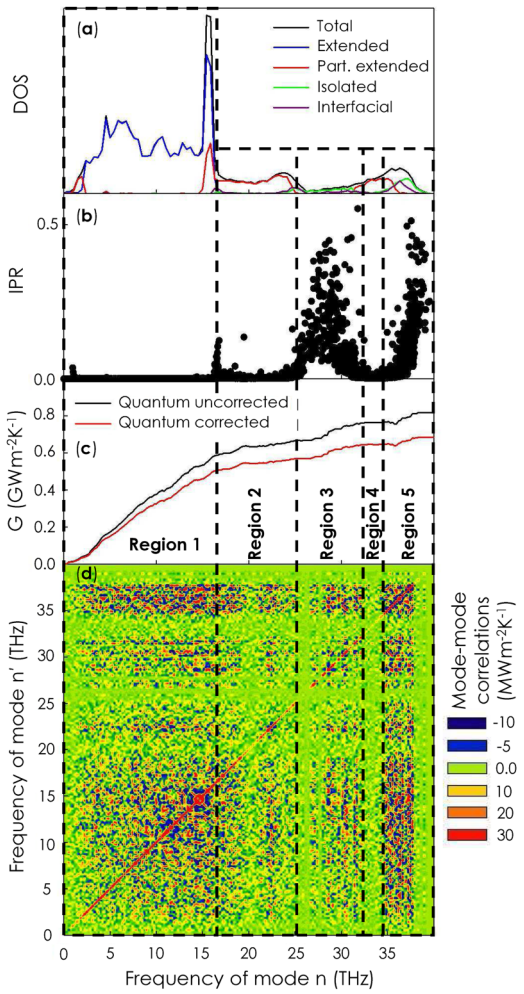

FIG. 4. DOS, IPR, and modal contributions to TIC for c-Si/a-SiO_2 interface at T = 600 K, which is a typical operating temperature in SOI technology.[11] (a) Total DOS and DOS for different mode classifications across the interface, (b) IPR for the vibrational modes in the system, (c) quantum-corrected and quantum-uncorrected TIC accumulation functions, and (d) 2D map showing the magnitudes of the correlations/interactions on the plane of two frequency axes. The values presented on the 2D map have units of MW m^{-2} K^{-1}.

of the localized modes, with the exclusion of low-frequency partially extended modes around ~1 THz, appear above ~16 THz, which is the maximum frequency of vibration for the Si side. The degree of localization can be quantified by calculating the inverse participation ratio (IPR)[28,46–48] [shown in Fig. 4(b)], which is a direct index for localization of vibrational states in a system. A value of IPR ~ 1 corresponds to a highly localized mode, and a value of IPR ~ 0 corresponds to a fully extended (i.e., delocalized) mode. As evident from Fig. 4(b), strongly localized modes (e.g., IPR > 0.2) are mainly distributed in two distinct frequency regions. The first region includes modes with frequencies from ~25 THz to ~33 THz, and the second region includes modes with frequencies larger than ~35 THz. The modes in these two regions are actually locons[46] on the a-SiO_2 side.[49] Based on the classification scheme of Gordiz and Henry,[9] the vibrational modes in these two regions would be considered interfacial modes, if they are close to the interface, but they would be considered isolated modes, if they do not have the majority of their energy in the interfacial region. Figure 4(c) shows the modal contributions in the form of a TIC accumulation function, and Fig. 4(d) represents the pairwise correlations between the modes in the system (see Ref. 9 for more details about the calculation). To better understand the contributions by different types of vibrations, we have divided the frequency domain into five different frequency regions, as shown in Fig. 4. The choice of these regions is based on the partial DOS [Fig. 4(a)] and the IPR [Fig. 4(b)]. As seen in Fig. 4, region 1 lies below the maximum frequency of Si (~16 THz), where >95% of the modes are extended. These extended modes contribute >70% to the TIC, and it is hypothesized that this is primarily through elastic interactions, due to the large values along the diagonal of the correlation map [Fig. 4(d), region 1], which indicate correlations with modes of the same frequency. Interactions between modes with the same frequency are usually associated with elastic interactions, because elastic interactions occur only between modes with the same frequency. Such a large contribution to TIC by extended modes can also be seen in other structures, such as InP/InGaAs,[42] where more than 70% of TIC originates from extended modes as well.

Regions 2 and 4 are mostly comprised of partially extended modes on the SiO_2 side. Despite the large number of modes in these regions (>30% of the total number of modes), their contribution to TIC is low (< 8%). On the other hand, although regions 3 and 5 do not have a large population of modes (< 5% of the total number of modes), their contribution to the TIC is substantial (>15%). The main contributing modes in these regions are interfacial modes that seem to be locons[28,46] on the a-SiO_2 structure. The correlation map in Fig. 4(d) shows that the interfacial modes in regions 3 and 5 have a very strong ability to interact (i.e., cross-correlate) with other modes to transfer their energy to the other side of the interface. The strong ability of interfacial modes to interact with the other modes in the system has been observed in the modal analysis of Si/Ge[29] and InP/InGaAs[42] interfaces as well.

To study the TIC at a different temperature, the classical modal contributions are first obtained from an MD simulation at that specific temperature. Then, the classically obtained modal contributions are rescaled using a quantum correction to the mode heat capacity, to capture an important aspect of the quantum effects present at that temperature. The details of the quantum correction have been reported in prior studies[9,31] and have been successfully used in temperature dependent predictions of thermal conductivity.[49–51] However, the effectiveness of such an approach for temperature dependent TIC predictions needs to be tested in comparison with experimental measurements. The values obtained for the total TIC before and after quantum correction are presented in Fig. 5 alongside the temperature dependent heat capacity values.[52] The relative contributions obtained by the classical MD-ICMA do not change much at higher temperatures, as Fig. 4, which corresponding to 600 K, shows less than 10% difference at other examined temperatures. Thus, the temperature dependence is dominated by the quantum effect on heat capacity. By comparing the temperature dependent TIC and heat capacity plots, the observed increase in TIC can be directly attributed to the increase in heat capacity, where modes with high frequencies (mostly on SiO_2 side) get excited at higher temperatures and start to contribute significantly to TIC. Specifically, the modal analysis results in Fig. 4 show that there is a significant contribution to the TIC from high frequency interfacial modes (regions 3 and 5). Thus, by raising the temperature, the heat capacity of these interfacial modes increases, and they start to contribute to the TIC. After the initial steady rise, the slope of $G(T)$ decreases around ~500 K. This is a consequence of partially extended modes in the range of ~20–25 THz starting to become excited. However, as was illustrated in Fig. 4, partially extended modes in this frequency region inherently do not significantly contribute to the TIC; thus, even though they get excited and contribute to the heat capacity, they only slightly change the value of the TIC.

In conclusion, we used equilibrium MD, LD, and ICMA to study the phonon contributions to the TIC at a crystalline Si and amorphous SiO_2 interface and found that the TIC is sufficiently large that interfacial resistance is highly unlikely to be the limiting heat dissipation factor in a typical industry-standard SOI wafer. We also compared the spatial distribution of the vibrational spectrum

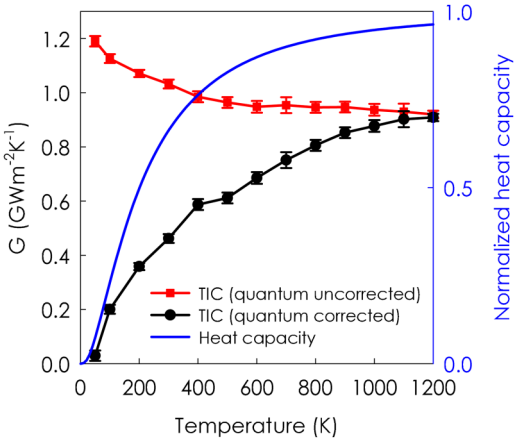

FIG. 5. Temperature dependent TIC before and after quantum correction (left y-axis) and normalized heat capacity (right y-axis) across the c-Si/a-SiO_2 interface structure.

with HERMES data and found good correspondence that provides initial evidence that experimentally confirms the existence of localized modes at an interface. Our modal analysis, using the ICMA method, showed that the majority of the TIC (>70%) comes from the extended modes, but localized interfacial modes also contribute significantly to the TIC (>15%), even though they comprise only a small portion (<5%) of the modes. These findings further substantiate the idea that the contribution of localized modes to thermal transport in systems with broken symmetries can be important and should not be neglected. Furthermore, due to the ease of fabrication of such structures, this system could prove to become a useful platform for testing the accuracy/validity of TIC theories, particularly if experimental measurements of the TIC can be obtained with certainty.

SUPPLEMENTARY MATERIAL

The supplementary material includes the needed explanations for (i) calculating the Gaussian weighted average of the kinetic energy of the atoms and (ii) calculating the harmonic and anharmonic energy distribution for each mode of vibration in the system.

ACKNOWLEDGMENTS

This work was supported by the Office of Naval Research (ONR) under a MURI program (Grant No. N00014-18-1-2429) and a National Science Foundation Career Award to A.H. (Award No. 1554050).

REFERENCES

[1]G. K. Celler, "SOI technology driving the 21st century ubiquitous electronics," ECS Trans. **19**, 3–14 (2009).
[2]S. Veeraraghavan and J. G. Fossum, "Short-channel effects in SOI MOSFETs," IEEE Trans. Electron Devices **36**, 522–528 (1989).
[3]M. Bruel, "Silicon on insulator material technology," Electron. Lett. **31**, 1201–1202 (1995).
[4]J.-P. Colinge, *Silicon-on-Insulator Technology: Materials to VLSI* (Springer Science & Business Media, 2004).
[5]D. G. Cahill *et al.*, "Nanoscale thermal transport. II. 2003–2012," Appl. Phys. Rev. **1**, 011305 (2014).
[6]F. VanGessel, J. Peng, and P. W. Chung, "A review of computational phononics: The bulk, interfaces, and surfaces," J. Mater. Sci. **53**, 5641–5683 (2018).
[7]B. Deng, A. Chernatynskiy, M. Khafizov, D. H. Hurley, and S. R. Phillpot, "Kapitza resistance of Si/SiO_2 interface," J. Appl. Phys. **115**, 084910 (2014).
[8]K. Gordiz and A. Henry, "A formalism for calculating the modal contributions to thermal interface conductance," New J. Phys. **17**, 103002 (2015).
[9]K. Gordiz and A. Henry, "Phonon transport at interfaces: Determining the correct modes of vibration," J. Appl. Phys. **119**, 015101 (2016).
[10]H. R. Seyf, K. Gordiz, F. DeAngelis, and A. Henry, "Using Green-Kubo modal analysis (GKMA) and interface conductance modal analysis (ICMA) to study phonon transport with molecular dynamics," J. Appl. Phys. **125**, 081101 (2019).
[11]H. Kappert, N. Kordas, S. Dreiner, U. Paschen, and R. Kokozinski, in *2015 IEEE International Symposium on Circuits and Systems (ISCAS)* (IEEE, 2015), pp. 1162–1165.
[12]K. T. Regner *et al.*, "Broadband phonon mean free path contributions to thermal conductivity measured using frequency domain thermoreflectance," Nat. Commun. **4**, 1640 (2013).
[13]M. G. Muraleedharan, A. Rohskopf, V. Yang, and A. Henry, "Phonon optimized interatomic potential for aluminum," AIP Adv. **7**, 125022 (2017).
[14]A. Rohskopf, H. R. Seyf, K. Gordiz, T. Tadano, and A. Henry, "Empirical interatomic potentials optimized for phonon properties," NPJ Comput. Mat. **3**, 27 (2017).
[15]J. Kimling, A. Philippi-Kobs, J. Jacobsohn, H. P. Oepen, and D. G. Cahill, "Thermal conductance of interfaces with amorphous SiO_2 measured by time-resolved magneto-optic kerr-effect thermometry," Phys. Rev. B **95**, 184305 (2017).
[16]H.-K. Lyeo and D. G. Cahill, "Thermal conductance of interfaces between highly dissimilar materials," Phys. Rev. B **73**, 144301 (2006).
[17]R. M. Costescu, M. A. Wall, and D. G. Cahill, "Thermal conductance of epitaxial interfaces," Phys. Rev. B **67**, 054302 (2003).
[18]B. C. Gundrum, D. G. Cahill, and R. S. Averback, "Thermal conductance of metal-metal interfaces," Phys. Rev. B **72**, 245426 (2005).
[19]S. S. Mahajan, G. Subbarayan, and B. G. Sammakia, "Estimating kapitza resistance between Si-SiO_2 interface using molecular dynamics simulations," IEEE Trans. Comp. Pack. Manuf. Technol. **1**, 1132–1139 (2011).
[20]E. Lampin, Q.-H. Nguyen, P. Francioso, and F. Cleri, "Thermal boundary resistance at silicon-silica interfaces by molecular dynamics simulations," Appl. Phys. Lett. **100**, 131906 (2012).
[21]C. M. Stanley, "Heat flow and Kapitza resistance across a Si|SiO_2 interface: A first principles study," doctoral dissertation (Texas Tech. University, 2018).
[22]C. M. Stanley and S. K. Estreicher, "Heat flow across an oxide layer in Si," Phys. Status Solidi (a) **214**, 1700204 (2017).
[23]J. Chen, G. Zhang, and B. Li, "Thermal contact resistance across nanoscale silicon dioxide and silicon interface," J. Appl. Phys. **112**, 064319 (2012).
[24]P. K. Schelling, S. R. Phillpot, and P. Keblinski, "Phonon wave-packet dynamics at semiconductor interfaces by molecular-dynamics simulation," Appl. Phys. Lett. **80**, 2484–2486 (2002).
[25]A. Minnich, "Advances in the measurement and computation of thermal phonon transport properties," J. Phys. Condens. Matter **27**, 053202 (2015).
[26]N. Mingo, in *Thermal Nanosystems and Nanomaterials* (Springer, 2009), pp. 63–94.
[27]O. L. Krivanek *et al.*, "Vibrational spectroscopy in the electron microscope," Nature **514**, 209 (2014).
[28]A. Giri, B. F. Donovan, and P. E. Hopkins, "Localization of vibrational modes leads to reduced thermal conductivity of amorphous heterostructures," Phys. Rev. Mat. **2** 056002 (2018).
[29]K. Gordiz and A. Henry, "Phonon transport at crystalline Si/Ge interfaces: The role of interfacial modes of vibration," Sci. Rep. **6** 23139 (2016).
[30]A. Giri *et al.*, "Interfacial defect vibrations enhance thermal transport in amorphous multilayers with ultrahigh thermal boundary conductance," Adv. Mater. **30**, 1804097 (2018).
[31]K. Gordiz, *Modal Decomposition of Thermal Conductance* (Georgia Institute of Technology, 2017).
[32]T. Feng *et al.*, "Spectral analysis of nonequilibrium molecular dynamics: Spectral phonon temperature and local nonequilibrium in thin films and across interfaces," Phys. Rev. B **95**, 195202 (2017).
[33]H. Zhao and J. Freund, "Lattice-dynamical calculation of phonon scattering at ideal Si–Ge interfaces," J. Appl. Phys. **97**, 024903 (2005).
[34]J. Tersoff, "Modeling solid-state chemistry: Interatomic potentials for multicomponent systems," Phys. Rev. B **39**, 5566 (1989).
[35]K. Sääskilahti, J. Oksanen, J. Tulkki, and S. Volz, "Spectral mapping of heat transfer mechanisms at liquid-solid interfaces," Phys. Rev. E **93**, 052141 (2016).
[36]T. Feng, Y. Zhong, J. Shi, and X. Ruan, "Unexpected high inelastic phonon transport across solid-solid interface: Modal nonequilibrium molecular dynamics simulations and Landauer analysis," Phys. Rev. B **99**, 045301 (2019).
[37]K. Gordiz and A. Henry, "Phonon transport at interfaces between different phases of silicon and germanium," J. Appl. Phys. **121**, 025102 (2017).
[38]J. D. Gale, "GULP: A computer program for the symmetry-adapted simulation of solids," J. Chem. Soc. Faraday Trans. **93**, 629–637 (1997).
[39]S. R. Elliott, *Physics of Amorphous Materials* (Longman Scientific & Technical; J. Wiley, 1990).

[40]K. Gordiz, D. J. Singh, and A. Henry, "Ensemble averaging vs. time averaging in molecular dynamics simulations of thermal conductivity," J. Appl. Phys. **117**, 045104 (2015).
[41]S. Plimpton, "Fast parallel algorithms for short-range molecular dynamics," J. Comput. Phys. **117**, 1–19 (1995).
[42]K. Gordiz and A. Henry, "Interface conductance modal analysis of lattice matched InGaAs/InP," Appl. Phys. Lett. **108**, 181606 (2016).
[43]M. G. Muraleedharan *et al.*, "Thermal interface conductance between aluminum and aluminum oxide: A rigorous test of atomistic level theories," preprint arXiv:1807.06631 (2018).
[44]K. Venkatraman, P. Rez, K. March, and P. A. Crozier, "The influence of surfaces and interfaces on high spatial resolution vibrational EELS from SiO_2," Microscopy **67**, i14–i23 (2018).
[45]C. W. Padgett and D. W. Brenner, "Influence of chemisorption on the thermal conductivity of single-wall carbon nanotubes," Nano Lett. **4**, 1051–1053 (2004).
[46]P. B. Allen, J. L. Feldman, J. Fabian, and F. Wooten, "Diffusons, locons and propagons: Character of atomic vibrations in amorphous Si," Philos. Mag. B **79**, 1715–1731 (1999).
[47]P. B. Allen and J. L. Feldman, "Thermal conductivity of disordered harmonic solids," Phys. Rev. B **48**, 12581 (1993).
[48]J. M. Larkin and A. J. McGaughey, "Predicting alloy vibrational mode properties using lattice dynamics calculations, molecular dynamics simulations, and the virtual crystal approximation," J. Appl. Phys. **114**, 023507 (2013).
[49]W. Lv and A. Henry, "Non-negligible contributions to thermal conductivity from localized modes in amorphous silicon dioxide," Sci. Rep. **6**, 35720 (2016).
[50]W. Lv and A. Henry, "Direct calculation of modal contributions to thermal conductivity via Green–Kubo modal analysis," New J. Phys. **18**, 013028 (2016).
[51]H. R. Seyf *et al.*, "Rethinking phonons: The issue of disorder," NPJ Comput. Mat. **3** 49 (2017).
[52]C. Kittel and P. McEuen, *Introduction to Solid State Physics* (Wiley, New York, 1986), Vol. 8.